www.czasopisma.pan.pl PAN POLSKA AKADEMIA NAUK www.journals.pan.pl

Arch. Metall. Mater. **70** (2025), 4, 1543-1551

DOI: https://doi.org/10.24425/amm.2025.156234

CHUNWANG LI[1*]

SIMULATION STUDY ON FOREIGN OBJECT DAMAGE IN TITANIUM ALLOY BLADES CAUSED BY CYLINDRICAL STEEL IMPACTS

Foreign object damage (FOD) is one of the main limiting factors for the life of aero-engine blades. In order to summarize the impact law and predict the damage gap caused by the impact of foreign objects on titanium alloy blades, the dynamic simulation calculation of foreign object damage at the inlet edge of an aero-engine guide vane was carried out with a specific blade as the research object, a cylindrical steel nail with high probability on the airport pavement as the foreign body and the most possible angle caused by the inlet flow field as the impact angle. The study found that: (i) The notch depth consists of two components: the initial depth at impact and the subsequent expansion due to centrifugal stress. (ii) The depth of the notch is always greater than the width. The maximum width of the notch is approximately equal to the cross-sectional diameter of the steel column. (iii) The relationship between notch depth and notch width is a quadratic function. (iv) The changes of notch depth with relative kinetic energy and steel column mass, and the changes of impact angle, maximum impact force and impact time with steel column mass are all power functions. With the increase of impact position, the relative kinetic energy of the steel column increases, and the change law is a quadratic function. (v) For the same foreign object, there is a critical value when the impact height increases. When the impact position is lower than it, the notch depth increases continuously. On the contrary, the notch depth decreases. Similarly, there is a critical value in the process of increasing relative kinetic energy. Smaller than it, the notch depth continues to increase, while larger than it, the notch depth continues to decrease. These findings provide data to support the diagnosis of blade damage under field conditions, and provide a theoretical basis for the design of blades against foreign object damage.

Keywords: Foreign object damage (FOD); Titanium alloy; blade; Steel column; Simulation

Symbol list

- E – Young's modulus (GPa)
- E_t – tangential modulus (GPa)
- ρ – mass density (kg/m^3)
- v – Poisson factor
- σ_0 – initial yield stress (MPa)
- β – hardening parameter
- C – strain rate parameter
- ε_f – failure plastic strain
- r – the radius of steel cylinder (mm)
- l – the length of steel cylinder (mm)
- m – the mass of foreign object (g)
- V_x – axial relative velocity (m/s)
- V_y – circumferential relative velocity (m/s)
- V_r – relative impact velocity (m/s)
- D – the depth of notch (mm)
- W – the width of notch (mm)
- E_r – the relative kinetic energy (J)
- θ – the included angle between impact direction and X-axis (°)
- F – the maximum impact force (N)
- t – the impact duration (10^{-5} s)
- h – the distance from the impact point to the blade root (mm)
- ξ – the distance from the impact point to the engine central axis (mm)

1. Introduction

Foreign object damage (FOD) of blades is very important to the safety of aircraft engines and the whole aircraft, and it is one of the main factors that limit the life of aircraft engine blades. Reducing fatigue of aircraft engine components caused by FOD is still one of the most important challenges facing

[1] XI'AN INTERNATIONAL UNIVERSITY, ENGINEERING COLLEGE, XI'AN, CHINA

* Corresponding author: li_chw@163.com

aviation engineers [1,2]. It is estimated that the costs caused by various types of FODs may have exceeded $4 billion every year [3]. It is found that the impact damage caused by ingestion of foreign objects is an important cause of high cycle fatigue (HCF) related failures in aircraft engines, and the impact of FOD on fatigue life is a key issue that needs to be considered in the design of Ti-6Al-4V alloy inlet guide blades [4]. Therefore, many reseachers have conducted extensive experimental or simulation studies on foreign object damage by replacing steel blocks with steel balls or steel cubes and sand rock with glass beads.

Yang [5] et al. used steel sphere to impact the standard thin plate specimen, and combined with numerical analysis to study the FOD characteristics of thin nickel-based superalloy plates. Results show that the crater has lager dimensions under high speed and elevated temperature. To study the residual stress caused by FOD, Matsunaga H [6] impacted Ti-6Al-4V alloy on the plane with steel balls at a speed of 180 m/s using an angle of 90° or 45°. It is found that the tensile residual stress that is more detrimental to fatigue strength is widely distributed inside the crater at the impact angle of 45°. Anuradha Nayak Majila [7] used an air cannon to launch steel balls with a diameter of 3.2 mm, causing them to impact Ti-6Al-4V alloy flat specimens vertically or at an angle of 60° at a speed of 300 m/s, and studied the effect of FOD on HCF. The results show that fatigue life reduced in FOD impacted samples and the debit in fatigue life is much larger than that for machined notch specimens. Zhu [8] used steel balls to impact TC4 titanium alloy plate specimens at angles of 30°, 60°, and 90° to study the initiation and propagation of cracks induced by FOD. The results reveal that all the cracks nucleate from the micronotches at the material pileup of FOD crater rim. Chen [9] used the finite element method to study the dynamic impact process of steel balls vertically impacting the side of Ti-6Al-4V thin plate, focusing on the influence of residual stress and stress concentration. It is found that the stress concentration factors primarily depend on the residual penetration. Besides, Chen et al. [10] conducted finite element simulation on the impact of hard spherical particles on thick elastic-plastic substrates. It is found that the maximum impact indentation can reduce the critical crack size of Ti-6Al-4V alloy blades by up to 60%.

Nicholas et al. [11] used a steel ball with a diameter of 3.18 mm to impact Ti-6Al-4V flat samples at a speed of 200 or 300 m/s, followed by tensile or torsional fatigue tests to determine its fatigue strength corresponding to 10^6 cycles. The most major finding is that stress relieved specimens were generally have higher fatigue strengths than those not relieved. Martinez et al. [12] used glass beads with 1 mm in diameter to impact simulated blades with a leading edge radius of 0.127 mm or 0.381 mm at a speed of 305 m/s along the vertical or 30° incident angle, to study the degradation degree of Ti-6Al-4V fatigue strength caused by FOD. The results show that fatigue strength degradation is higher for the 30° impacts than for the 0° impacts. Ruschau et al. [13] used glass spheres with 1.0mm in diameter to impact the specimen replicated typical fan blade leading edges, studying the effect of impact angle on fatigue strength. It is found that off-angle impacts is more detrimental than head-on (0°) impacts.

Harish Ra [14] et al. used GCr15 stainless steel balls to impact leading-edge specimen (TC11 titanium alloy) by varying speeds to predict the possible location of crack initiation at different impact speeds, and the stress concentration factor has also been calculated. The results show that three parameters related with foreign object damage, such as stress raisers /concentration at the impact location, residual stress, and distortion of micro-structure, lead to degradation of the fatigue strength of the specimen. Zheng Guang-dong [15] et al. used steel balls to simulate the leading edge of blades, and then carried out high-cycle fatigue tests to study the effects of notch residual stress distribution on the initiation of fatigue cracks and fatigue limit. It is found that the notch size caused by impact increases with the increase of impact energy.

Nowell et al. [16] used a cube as a hard object to obtain tooth impact damage at a speed of 250 m/s, and analyzed the relationship between damage size, impact angle and fatigue strength. It is shown that damage depth has a significant effect on fatigue strength. Ding et al. [17] used air cannon to launch steel cubes a to study the interaction between FOD and fatigue behavior of specimens. The results indicated that residual stresses significantly affected both the development of crack front shape and the fatigue life. Davis et al. [18] used an explicit-implicit mixed finite element method for numerical simulation to study the residual stress relaxation caused by a cubic block with a side length of 3 mm impacting a Ti-6Al-4V flat plate specimen at a speed of 200 m/s. The results show that relaxation and redistribution of the residual stresses are predicted to occur during cyclic loading. Frankel et al. [19] used cubic blocks with a side length of 3 mm to impact the side surface of Ti-6Al-4V flat standard specimens and the thin leading edge of prefabricated intake leading edge flat specimens, and compared the effects of FOD on thick planes and thin leading edges. It is found that the stress field for cube-edge impact on a thin leading edge give rise to larger compressive stresses immediately beneath the notch compared to those for the same cube-edge impact on a flat face.

Oakley et al. [20] used a cube with a side length of 3.2 mm to impact the leading edge of a Ti-6Al-4V "blade shaped" specimen at a speed of 180 m/s, obtaining a V-shaped notch with a depth of 0.1 to 1.1 mm. Then they conducted a combined high and low cycle fatigue test to study the residual fatigue life of aircraft engine blades after FOD. The research suggests a region where cracks may arrest as far as HCF loading are concerned, but continue to propagate under LCF. Lin et al. [21] analyzed the fatigue crack propagation in complex residual stress fields under combined high and low cycle fatigue conditions, by using hardened steel cube with a side length of 3 mm to impact Ti-6Al-4V simulated blade specimen treated with laser shock peening, and impacted it head-on at a speed of 200 m/s or at a 45 degree angle at a speed of 250 m/s. The results indicate that residual stresses due to LSP and FOD play a key role in influencing the fatigue crack growth behaviour. Zabeen et al. [22] also used cubes to impact the leading edge of blades machined on Ti-6Al-4V flat specimens

to investigate the effect of laser shock strengthening on residual stresses. It is shown that the FOD notch created by 45° impact was asymmetric in shape and smaller in depth compared to that created at 0°. Spanrad et al. [23] machined the leading edge of blades on Ti-6Al-4V flat specimens and impacted the blade leading edge with steel balls and cubes after and without laser shock strengthening. It is found that the laser shock strengthening delayed crack initiation under the same damage characteristics.

Previous studies mainly have considered spherical [5-15] and cubic [16-23] objects; However, cylindrical foreign objects – common on airport pavements – remain insufficiently investigated. This shows that it is not only necessary but also urgent to study the FOD of columnar metal to aero-engine blades. Moreover, the specimens used are either flat plates [5-10,16-19] or only the leading edges machined at the inlet side [11-15,20-23], but they are not real blades. The impact direction is along the preset angle, and the most probable speed and angle are not determined according to the specific model and working condition of the engine.The research content also focuses on the influence of damage notch on fatigue, but there is little research on the corresponding relationship between the size of damage notch and the nature of foreign objects and its law, let alone the research on the damage law of specific blade profile. This study just fills these gaps.

In this paper, the inlet guide vane of a specific aero-engine is taken as the research object. According to the flow field analysis, the velocity and direction of steel cylinders of different sizes relative to the moving blades are obtained [24], and then the impact process is dynamically simulated, and the relationship between the size and motion state of foreign objects and the impact effect is studied. The conclusions obtained can not only guide the anti-foreign damage design of this type of blade, but also have certain theoretical significance for making the criteria for judging scrapping and repairing damaged blades.

2. Simulation of foreign object impact at the Specific height

2.1. FOD Calculation model for the Specific height

The material of the first-stage rotor blade of the aero-engine compressor studied is titanium alloy, which's and cylindrical steel's material and calculation parameters are listed in TABLE 1 [25]. And their geometric model and installation state are shown in Figs. 1 and 2. The model adopts cylindrical coordinates, with the central axis of the engine as the X-axis, the airflow direction as the positive direction, the circumferential axis as the Y-axis, and the radial axis as the Z-axis. When the engine is working, the maximum angular velocity of the first-stage rotor blade is 1036 rad/s [26]. At this time, the airflow speed and the speed of foreign objects relative to the blade reach the maximum. When the foreign objects with the same size and material impact the blade, the damage is also the most serious. Therefore, this working condition is chosen as the research state.

TABLE 1

Material and calculation parameters [25]

Material	E (GPa)	E_t (GPa)	ρ (kg/m^3)	v	σ_0 (MPa)	β	C	P	ε_f
Titainum alloy	112.5	1.125	4500	0.33	950	0	0	0	0.20
Steel	200	2	7800	0.30	1620	0	0	0	0.06

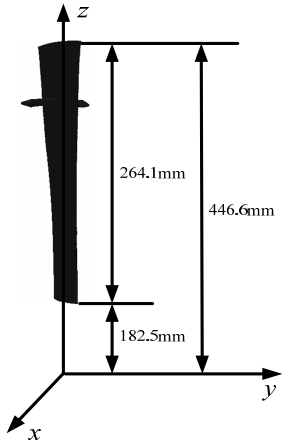

Fig. 1. Geometric model and installation position

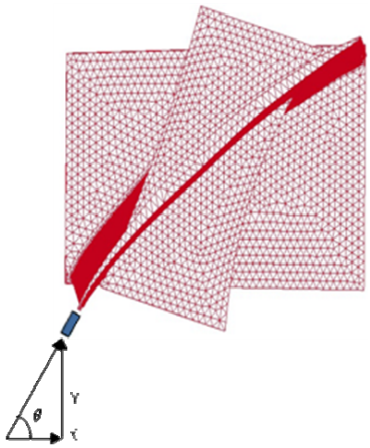

Fig. 2. Schematic diagram of FOD

2.2. Results of the impact damage

In the process of dynamic simulation, the centrifugal stress distribution in the rotating blade is calculated by using the implicit solver of the ANSYS simulation platform. Then the blade model with centrifugal prestress is imported into ANSYS/LS-DYNA for explicit dynamic analysis. Finally, the FOD notch morphology of the blade considering the influence of centrifugal prestress is obtained.

2.3. Result analysis of foreign object damage

On one occasion, the leading edge of the rotor blade studied was damaged by foreign objects, and the impact point was

located at 210.35 mm from the blade root and 392.85 mm from the engine shaft. In this paper, this point is selected as the impact point to study the law of damage notch caused by the impact of steel columns with different sizes on the leading edge of the blade at different speeds. The circumferential velocity corresponding to this point is 407 m/s.

In order to comprehensively reflect various factors affecting the FOD, the concept of "relative kinetic energy" and the calculation method of impact angle in reference [24] are followed. The relative kinetic energy and impact angle of steel columns with different sizes and speeds are shown in TABLE 2.

TABLE 2

Simulation Results of Steel Cylinders Impacting on Blades

r	0.3	0.6	0.9	1.2	1.4	1.7	2.0
l	2	4	6	8	10	12	14
m	0.004	0.03	0.11	0.26	0.51	0.88	1.4
V_x	183.1	158.6	146.2	138.3	132.7	128.4	125.0
V_r	446.3	436.8	432.5	429.9	428.1	426.8	425.8
D	1.4	5.7	9.1	11.6	14.8	15.8	19.0
W	0.6	1.3	1.9	2.6	3.0	3.6	4.2
E_r	0.432	3.31	11.0	25.7	43.3	76.2	122.0
θ	65.78	68.71	70.24	71.23	71.94	72.49	72.92
F	203	239.0	504.0	773.0	992.0	1320	1730
t	1.5	4.0	5.0	6.5	7.5	8.5	10.0

In the impact process, both steel columns and blades undergo plastic deformation. When the equivalent plastic strain is greater than its failure plastic strain, the steel columns will crack. When the equivalent plastic strain of a blade is larger than its failure plastic strain, a notch will be produced. At the same velocity (kinetic energy), the different shapes and sizes of notches and the different impact duration all reflect the influence of foreign object shape on blade impact damage. The concrete calculation results are shown in Figs. 3-4 and TABLE 2. After

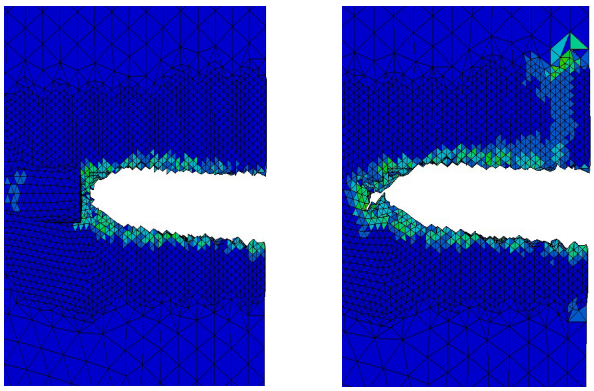

(a) Notch morphology at the end of impact (b) Stable notch morphology at the final moment

Fig. 3. Calculation results of steel columns impacting on blades with r = 1.4 mm, l = 10 mm

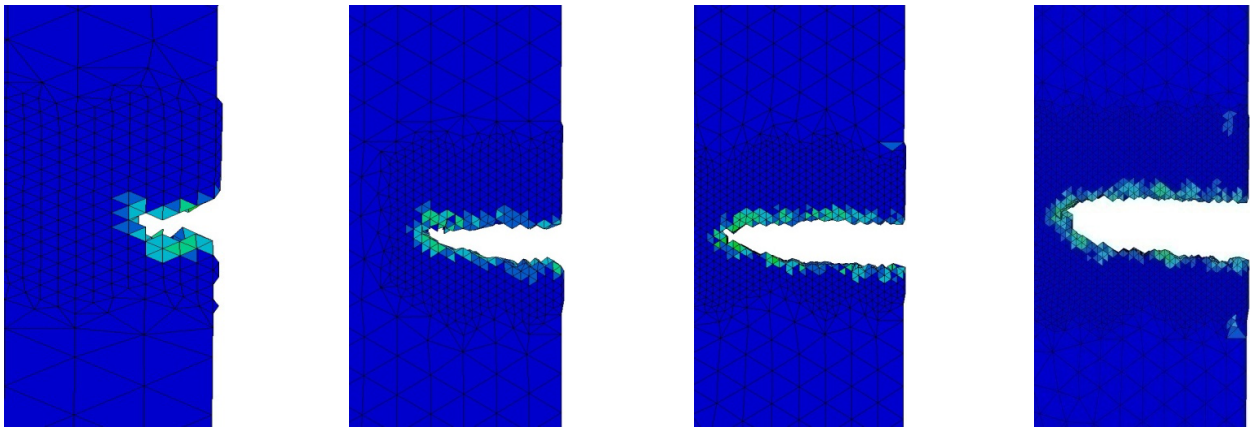

(a) r = 0.3 mm, l = 2 mm (b) r = 0.6 mm, l = 4 mm (c) r = 0.9 mm, l = 6 mm (d) r = 1.2 mm, l = 8 mm

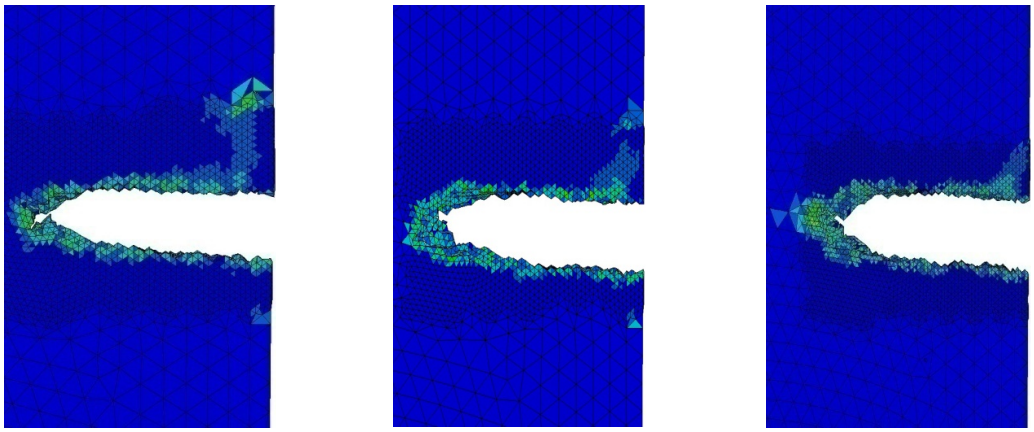

(e) r = 1.4 mm, l = 10 mm (f) r = 1.7 mm, l = 12 mm (g) r = 2.0 mm, l = 14 mm

Fig. 4. Stable notch morphology of blades impacted by steel columns of different sizes

carefully studying the calculated data and damage effect diagram, it is found that:

(1) The maximum width of the impact damage notch is equal to about twice the radius ($w \approx 2r$). According to this relationship, the radius of the columns can be estimated by the width of the notch, that is, the size of the columns along the radial direction (Z-axis direction). The reason for this result is that the impact direction of the foreign object is perpendicular to the radial direction of the blade.

(2) Although the steel column is separated from the blade after the impact, the damage notch will be further enlarged under the combined action of impact stress field and rotating centrifugal stress. Sometimes, in the process of rotating vibration of the blade, micro-cracks will also occur at the root of the notch, as shown in Fig. 3. The final stabilized notch depths are shown in Table 2 and Fig. 4, which include two components: the initial depth at impact and the subsequent expansion due to centrifugal stress.

(3) When the steel columns impact the leading edge of the guiding rotor, the relationship between D and W is always $D > W$. This conclusion provides a basis for qualitative judgment of the types of foreign objects that cause notch. Further fitting of data of D and W in TABLE 2, it can be obtained that:

$$D = -0.364W^2 + 6.521W - 2.259 \tag{1}$$

The results show that the change in notch depth with width is a quadratic function. The curve is as shown in Fig. 5 as well.

(4) Fitting the data D and E in TABLE 2, it can be got that.

$$D = 10.46E^{0.1914} - 7.494 \tag{2}$$

It is indicated that the change of notch depth with the relative kinetic energy of steel column is a power function, and D increases with the increase of E. The curve is shown in Fig. 6.

(5) Fitting the data D and m in TABLE 2, it can be got that.

$$D = 25.50m^{0.1719} - 8.394 \tag{3}$$

It is indicated that the variation law of notch depth with the quality of steel column is also a power function, and D increases with the increase of m, as shown in Fig. 7.

(6) Fitting the data θ and m in TABLE 2, it can be got that:

$$\theta = 4320.4m^{0.00028} - 4247.7 \tag{4}$$

It can be seen that the variation law of impact angle with the mass of steel column is still a power function, θ increases with the increase of m, and the curve is shown in Fig. 8.

(7) Fitting the data F and m in TABLE 2, it can be got that:

$$F = 1312.8m^{0.5774} + 122.82 \tag{5}$$

Therefore, the variation of the maximum impact force with the mass of steel column is still a power function, and F increases with the increase of m, as shown in Fig. 9.

(8) Fitting the data t and m in TABLE 2, it can be got that:

$$t = 11.46m^{0.1838} - 2.463 \tag{6}$$

Therefore, the change rule of impact duration with the mass of the steel column is also a power function, and t increases with the increase of m, as shown in Fig. 10.

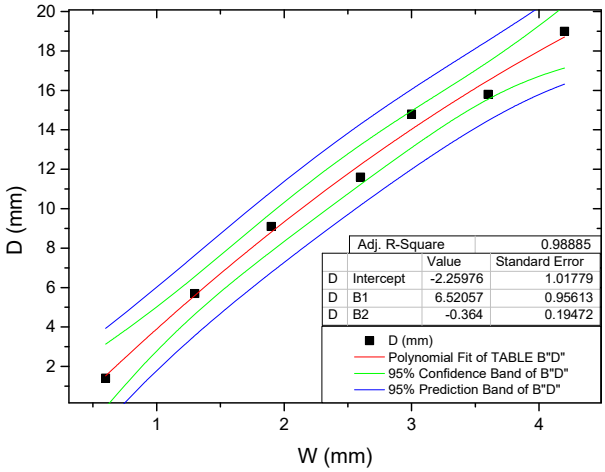

Fig. 5. The curve of notch depth varying with width

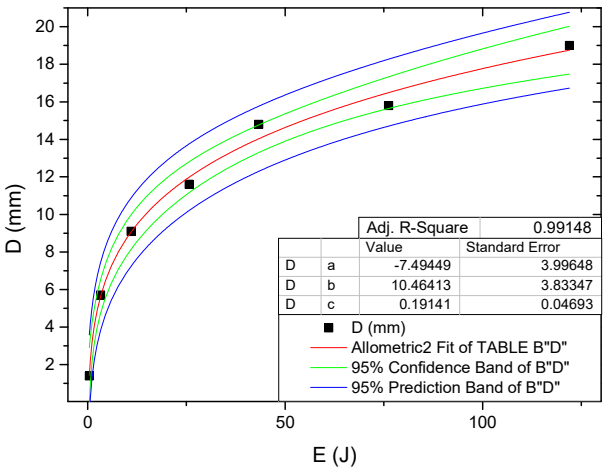

Fig. 6. The curve of notch depth varying with relative kinetic energy

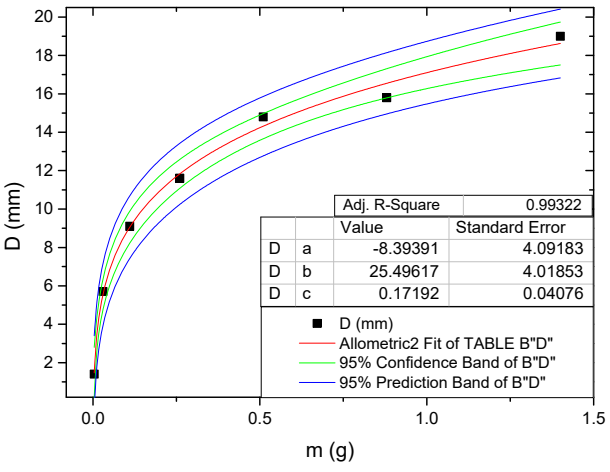

Fig. 7. The curve of notch depth varying with width

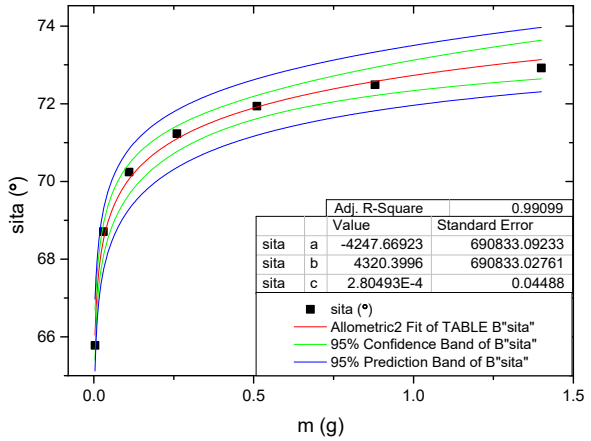

Fig. 8. The curve of the impact angle varying with the mass of the steel column

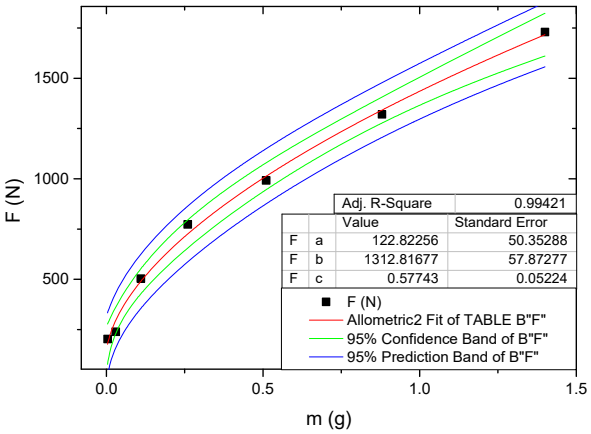

Fig. 9. The curve of maximum impact force varying with the mass of steel column

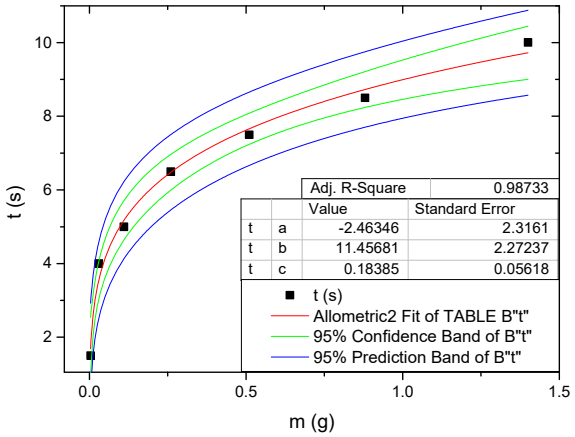

Fig. 10. The curve of the impact duration varying with the mass of the steel column

3. Impact simulation at different heights

3.1. Simulation model of foreign object damage

In order to study the variation law of damage with the height of the impact point, eight impact points were selected for simulation analysis. From the root of the blade, each impact point was 30 mm higher than the previous one. The selected steel nail has a radius of 0.6 mm, a length of 4mm, and an axial relative velocity of 158.6 m/s. The circumferential velocity at different blade heights is obtained by multiplying the rotational angular velocity of 1036 rad/s [26] by the distance between the impact point and the central shaft of the engine. The calculation model is shown in Figs. 1-2.

3.2. Results and analyses of impacts at different heights

The results of impacts at different heights are shown in TABLE 3.

TABLE 3

The results of impacts at different heights

h	0.0	30	60	90	120	150	180	210
ξ	183.0	212.45	242.47	272.49	302.51	332.53	362.55	392.47
V_y	189.1	220.1	251.2	282.3	313.4	344.5	375.6	407.0
V_r	246.8	271.3	397.1	323.8	351.2	379.3	407.7	436.8
D	1.6	2.8	3.6	4.1	5.2	6.4	5.9	5.7
W	1.4	1.4	1.5	1.5	1.5	1.5	1.5	1.5
E_r	1.06	1.28	1.53	1.82	2.14	2.50	2.89	3.31
θ	50.01	54.22	57.73	60.67	63.16	65.28	67.11	68.71
t	4.0	4.0	3.5	3.5	3.5	3.5	3.5	4.0

By analyzing the data in TABLE 3, we can get the following conslusions.

(1) As mentioned above, after the impact, under the joint action of impact stress field and rotating centrifugal stress field, the notch will continue to expand. At this time, the depth expansion of notch at different heights is also affected by the impact angle and the twist angle of blade profile.
Fitting the data D and h in TABLE 3, the relationship between the damage depth and the impact position can be obtained as follows.

$$D = e^{(-4.184\times10^{-5}h^2 + 0.0146h + 0.5284)} \tag{7}$$

The corresponding curve is shown in Fig. 11. It can be seen that the depth of damage caused by screws generally increases with the increase of the distance from the impact point to the blade root. However, there is a critical height (150 mm). When the impact position is higher than that, the notch depth decreases slightly with the increase of the impact height.

(2) Fitting the data D and E in TABLE 3, the relationship between damage depth and relative kinetic energy is obtained as follows.

$$D = e^{(-0.3985E^2 + 2.215E - 1.244)} \tag{8}$$

The corresponding curve is shown in Fig. 12. Therefore, the depth of impact damage caused by screws generally

increases with the increase of relative kinetic energy. However, there is also a critical relative kinetic energy of 2.50 J. When the relative kinetic energy is larger than this value, the damage depth decreases slightly with the increase of relative kinetic energy.

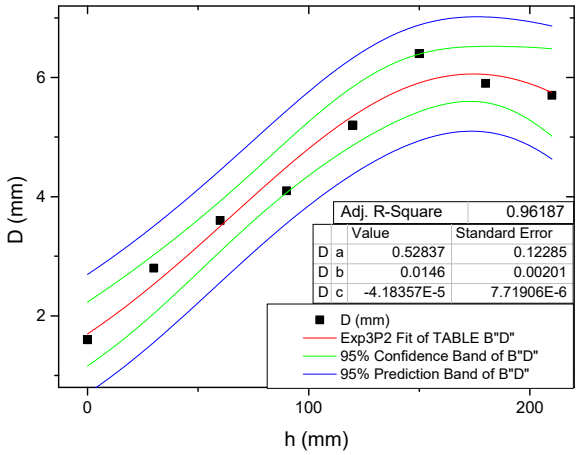

Fig. 11. The curve of the notch depth varying with the height of the impact point

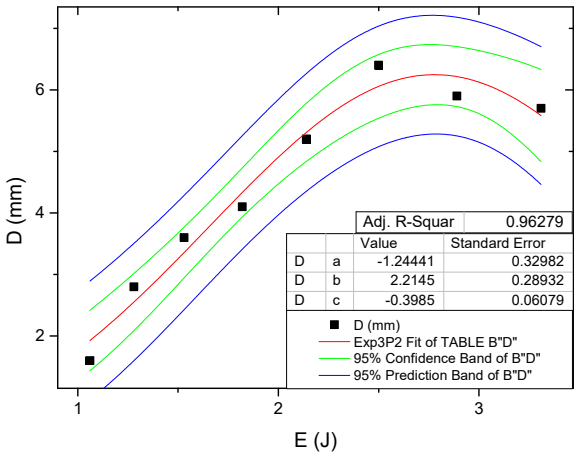

Fig. 12. The curve of the notch depth varying with the relative kinetic energy

(3) Fitting the data E and h in TABLE 3, the relative kinetic energy of the screw varies with the impact position as follows:

$$E = 1.898\times10^{-5}h^2 + 0.00674h + 1.06 \quad (9)$$

This relationship is a quadratic function, as shown in Fig. 13. With the increase of impact position, the corresponding circumferential velocity increases, which leads to the increase of relative kinetic energy of foreign objects.

4. Conclusions

In this paper, the impact damage of foreign objects such as steel nails on the first-stage rotor blades of an aero-engine

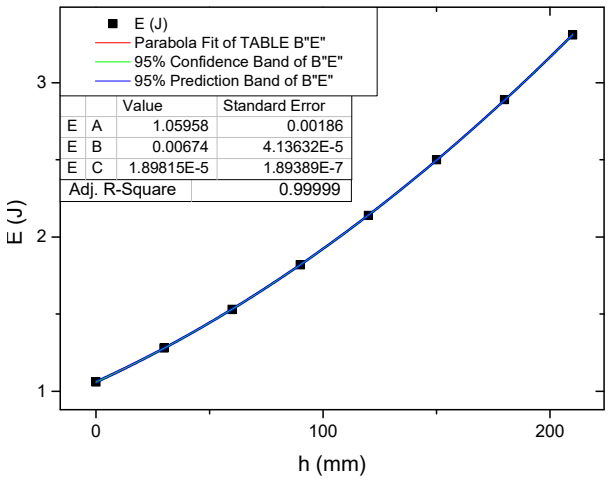

Fig. 13. The curve of the relative kinetic energy varying with the height of the impact point

compressor is simulated and analyzed, and it is found that.

(1) When the screw hits the inlet edge of the blade, the relationship between D and W is always $D > W$. The maximum width of the impact damage notch is equal to about twice the radius ($w \approx 2r$). This result reflects the size of the foreign object along the radial direction (Z axis direction).

(2) The notch depth consists of two components: the initial depth at impact and the subsequent expansion due to centrifugal stress.

(3) For a certain impact point, the relationship between notch depth and notch width is a quadratic function. The relationship between notch depth and relative kinetic energy, screw mass, and the relationship between impact angle, maximum impact force, impact duration and screw mass are all power functions. Notch depth increases with increasing notch width; notch depth increases with increasing relative kinetic energy and screw mass; impact angle, maximum impact force and impact duration increase with increasing screw mass.

(4) When the impact point is rising, the damage depth caused by the screw generally increases with the increase of the distance from the impact point to the blade root. However, there is a critical height of 150 mm. When the impact position is higher than this height, the depth of the notch depth decreases slightly with the increase of the impact height.

(5) With the rises of the impact position, the corresponding circumferential velocity increases, which generally leads to the increase of the relative kinetic energy of the screw and the depth of the notch. However, there is a critical relative kinetic energy of 2.50 J. When the relative kinetic energy is greater than this value, the damage depth decreases slightly with the increase of the relative kinetic energy.

In this paper, some meaningful work has been done in FOD simulation analysis of aero-engine blades, and some useful conclusions have been obtained. Generally speaking, the conclusions shold be verified by experiments. At the same time, these

equations need to be generalized in actual damage identification. However, it's a pity that we haven't carried out the experiment yet, which will be our next task.

The conclusions obtained in this paper will provide data to support judging the causes or symptoms of blade accidents in the outfield, and provide theoretical basis for the fatigue design of blades against FOD.

Acknowledgments

The authors gratefully acknowledge the financial support of the National Natural Science Foundation of China (No. 51575524 and No. 51601221), Natural Science Basis Research Plan in Shaanxi Province of China (No. 2025JC-YBMS-777), Scientific Research Project of Youth Innovation Team of Shaanxi Provincial Department of Education (grant no. 24JP162).

REFERENCE

[1] J.O. Peters, B.L. Boyce, A.W. Thompson, R.O. Ritchie, O. Roder, Role of Foreign Object Damage on Thresholds for High-Cycle Fatigue in Ti-6Al-4V. Metallurgical and Materials Transactions; A; Physical Metallurgy and Materials Science **31** (6), 1571-1583 (2000).

[2] Yoichi Yamashita, Yusuke Ueda, Hiroshi Kuroki, Masaharu Shinozaki, Fatigue life prediction of small notched Ti-6Al-4V specimens using critical distance. Engineering Fracture Mechanics **77** (9), 1439-1453 (2010).

[3] X. Chen, Foreign object damage on the leading edge of a thin blade. Mechanics of Materials **37** (4), 447-457 (2005).

[4] J.O. Peters, R.O. Ritchie, Foreign-object damage and high-cycle fatigue of Ti-6Al-4V. Materials Science and Engineering A: Structural Materials: Properties, Microstructure and Processing 319-321, 597-601 (2001).

[5] Weizhu Yang, Haowei Yang, Jianjun Liu, Yan Zeng, Xinmei Wang, Lei Li, Foreign object damage characteristics of a thin nickel-based superalloy plate at room and high temperatures. Thin–Walled Structures **202**, 1-21 (2024).

[6] Hisao Matsunaga, Effect of impact velocity and impact angle on residual stress fields caused by foreign object damage. Strain **56** (5) e12367-e12367 (2020).

[7] Anuradha Nayak Majila, S. Ramachandra, S.L. Mannan, D. Chandru Fernando, S.N. Narendrababu, Influence of Foreign Object Damage on High Cycle Fatigue of Ti-6Al-4V Alloy. Transactions of the Indian Institute of Metals, 2015.

[8] Lei Zhu, Xuteng Hu, Rong Jiang, Yingdong Song, Shoudao Qu, Experimental investigation of small fatigue crack growth due to foreign object damage in titanium alloy TC4. Materials Science & Engineering A **739**, 214-224 (2019).

[9] Xi Chen, Foreign object damage on the leading edge of a thin blade. Mechanics of Materials **37** (4), 447-457 (2005).

[10] Xi Chen, John W. Hutchinson, Foreign object damage and fatigue crack threshold: Cracking outside shallow indents, International Journal of Fracture **107** (1), 31-51 (2001).

[11] Ted Nicholas, Steven R. Thompson, William J. Porter, Dennis J. Buchanan, Comparison of fatigue limit strength of Ti-6Al-4V in tension and torsion after real and simulated foreign object damage. International Journal of Fatigue **27** (10), 1637-1643 (2005).

[12] Christine M. Martinez, Daniel Eylon, Theodore Nicholas, Steven R. Thompson, John J. Ruschau, Janine Birkbeck, William J. Porter, Effects of ballistic impact damage on fatigue crack initiation in Ti-6Al-4V simulated engine blades. Materials Science and Engineering A **325** (1), 465-477(2002).

[13] John J. Ruschau, Theodore Nicholas, Steven R. Thompson, Influence of foreign object damage (FOD) on the fatigue life of simulated Ti-6Al-4V airfoils. International Journal of Impact Engineering **25**, 233-250 (2001).

[14] Harish Ra, D. Shivalingappaa, H.G. Hanumantharajub, Raghavendra N. Ra, Impact of foreign object damage on the leading edge of TC11 titanium alloy aeroengine blade like specimen. Australian Journal of Mechanical Engineering **21** (4), 1115-1124 (2023).

[15] Zheng Guang-dong, Zhao Zhen-hua, Huang Zong-zheng, Li Jian, Mi Dong, Guo Xiao-jun, Lu Kai-nan, Chen Wei, Fatigue Limit and Predication of Foreign Object Damage of TC4 Titanium Alloy. Journal of Propulsion Technology **44** (11), 2206005-1–2206005-9 (2023).

[16] D. Nowell, P. Duó, I. F. Stewart, Prediction of fatigue performance in gas turbine blades after foreign object damage. International Journal of Fatigue **25** (9), 963-969 (2003).

[17] J. Ding, R.F. Hall, J. Byrne, J.Tong, Fatigue crack growth from foreign object damage under combined low and high cycle loading. Part 1: experimental studies, International Journal of Fatigue **29** (1), 1339-1349(2007).

[18] T. Davis, J. Ding, W. Sun, S.B. Leen, Computational simulation of the relaxation of local stresses due to foreign object damage under cyclic loading, Proceedings of the Institution of Mechanical Engineers. Part L: Journal of Materials Design and Applications **224** (L2), 41-50 (2010).

[19] P.G. Frankel, P.J. Withers, M. Preuss, H.-T. Wang, J. Tong, D. Rugg, Residual stress fields after FOD impact on flat and aerofoil-shaped leading edges. Mechanics of Materials **55** (1), 130-145 (2012).

[20] S.Y. Oakley, D. Nowell, Prediction of the combined high- and low-cycle fatigue performance of gas turbine blades after foreign object damage. International Journal of Fatigue **29** (1), 69-80 (2007).

[21] B. Lin, C. Lupton, S. Spanrad, J. Schofield, J. Tong, Fatigue crack growth in laser-shock-peened Ti-6Al-4V aerofoil specimens due to foreign object damage. International Journal of Fatigue **59** (1), 23-33 (2014).

[22] S. Zabeen, M.Preuss, P.J.Withers, Residual stresses caused by head-on and 30° foreign object damage for a laser shock peened Ti-6Al-4V alloy aerofoil. Materials Science & Engineering A **560**, 518-527 (2013).

[23] S. Spanrad, J. Tong, Characterisation of foreign object damage (FOD) and early fatigue crack growth in laser shock peened Ti-6Al-4V aerofoil specimens. Materials Science and Engineering A **528** (4-5), 2128-2136 (2011).

[24] C.W. Li, Z. Miao, B.Y. Yang, Z.P. Zhang, L.Y. Zhang, Study on Foreign Object Damage Law of Titanium Alloy Blade of an Aero-Engine Impacted by Sandstone. Strength of Materials **54** (2), 292-301 (2022).

[25] Zhu Guanfang, Li Chunwang, Wu Xiaoliang, Li Jing, Zhang Zhongping, The TC4 alloys Parameter Inversion of Cowper-Symonds Model. Chinese Journal of Applied Mechanics **36** (4), 945-950 (2019).

[26] State-run hongqi machinery factory, Technical specification of XXX engine, Xi'an, Shaanxi, DC: Author, 1981.

Appendix: Grid size and number

In the simulation calculation, the unit size and grid number of steel cylinders with different sizes and corresponding blades are shown in TABLE A. and TABLE B. The meanings of each symbol are: N_s – the grid number of steel cylinder, N_b – the grid number of blade. When dividing the grid, the side length of the blade grid is fixed at 1.55 mm, and then the impact part of the blade is partially refined.

TABLE A

Grid Number of the Model Impactted at the Same Position

r	0.3	0.6	0.9	1.2	1.4	1.7	2.0
l	2	4	6	8	10	12	14
N_s	4310	4270	4296	4305	4579	4313	4224
N_b	154363	174984	175692	182460	188953	186144	199458

TABLE B

Grid number of the impacting model at different heights

S	1	2	3	4	5	6	7	8
h	0	30	60	90	120	150	180	210
N_s	4332	4245	4302	4324	4381	4331	4316	4279
N_b	174195	172585	183140	163711	170290	181197	158387	157886